A Performance Comparison of Different Rotor Types for High-Speed Induction Motors

Daniel Tunc MCGUINESS, Mehmet Onur GULBAHCE, and Derya Ahmet KOCABAS

Dept. of Electrical Engineering, Istanbul Technical University, Istanbul, Turkey
mcguiness@itu.edu.tr, ogulbahce@itu.edu.tr, kocabasde@itu.edu.tr

Abstract

In recent years, improvements in the manufacturing, transport and process industries have brought about an increase in the optimum operating speed for drive systems. In this respect, the recently developed, high-speed, gearless or direct electrical drives are currently very popular, because of the reduction in the total structural volume of the drive system.

In this study, the performances of four high-speed induction motors with different types of rotor, i.e., cage, smooth solid, slitted solid and coated solid, were examined in cases where the geometrical size is kept constant. All the motors with different rotor types have a particular number of turns per phase in their slots, which is arranged to obtain the same rated current value when compared with the reference, conventional cage-induction machine. In order to compare the performance characteristics brought about by the change in the rotor's structure for different numbers of turns, all the induction motors were analyzed with the finite-element method (FEM). Using a coating with a high electrical resistivity was shown to increase the torque output. It was also clear that cutting the rotor in the axial direction increases both the flux penetration and the efficiency.

Keywords—induction motor; cage rotor; smooth solid rotor; slitted solid rotor; coated solid rotor, finite-element method

1. Introduction

Polyphase induction motors (IMs) have clear advantages in terms of their efficiency and the simplicity of their construction. Furthermore, by using different types of rotor construction, a variety of torque characteristics can be achieved. The most common type of IM is the squirrel-cage IM. Such a motor consists of a steel cylinder, with the slots being filled with mostly aluminum conductors. Although this cage-induction machine has widespread use in industrial applications, the weakness of its structure for high-speed implementation limits its use to the current range of applications. Depending on the structural complexity, the rotor design has several constraints that limit its operation in terms of angular speed, since the rotor cannot withstand the large rotational stresses caused by the high circumferential velocity of the rotor. Practical studies have shown that a squirrel-cage rotor cannot operate at speeds of 50,000 rpm [1].

When a high-speed application is targeted, a solid rotor is by far the better choice. The motors with solid rotors have advantages over other types of induction motor in terms of mechanical strength and structural simplicity, as well as being easier to manufacture [2]. For this reason, solid rotors are superior to conventional cage-rotor structures in terms of their ability to operate in extremely high-speed applications and their durability with respect to high thermal stresses that ensure low levels of vibrations under all operating conditions [3].

The simplest rotor type for solid rotors is the smooth, steel cylinder. [4] It is cheap and easy to manufacture such a solid rotor because of its basic geometrical shape. The simple structure means it has the best mechanical, fluid and thermal dynamics possible in an electrical rotor when compared to other rotors [4]. However, its electromagnetic properties are not as good as the other types, for example, its slip value is much higher for same load torque. As a result of the skin effect, eddy currents travel around the surface of the rotor, and travelling eddy currents at the surface of a ferromagnetic rotor material push the induced magnetic field towards the outer layer of the rotor. This means that the depth of the magnetic flux's penetration into the rotor is very shallow. The magnetic flux and the torque-producing eddy currents are concentrated on the surface layer and the interior part of the rotor becomes electrically inert [3].

When designing a solid rotor, special care must be paid to eliminating the air-gap harmonics that contribute a major part to the rotor losses, predominantly on the surface of the rotor [3]. In order to minimize the rotor losses, there are different rotor designs. One of the most common rotor types is the axially slitted rotor, which helps to decrease the effects of the rotor losses caused by the air-gap harmonics [5]. The fundamental component of the magnetic flux penetrates deeper into the rotor, thereby improving the electromagnetic performance of the motor in this slitted geometry. In order to obtain the optimum electromagnetic performance with the slitted rotor, the slit width must be 1.5 mm and the slit depth must be half of the rotor's radius [6]. The main drawbacks of an axially slitted rotor are a reduction in the mechanical strength and an increase in the audible noise, the manufacturing costs and the air-friction losses. Since these frictional losses increase as a square of the speed, a smooth cylinder is the most favorable choice for high-speed drive applications [2].

The other method to reduce rotor losses is using a conductive coating around the rotor, acting as a low-pass filter for the air-gap harmonics in a high-speed drive application. The coating decreases the impact caused by the air-gap harmonics, while increasing the motor's electromagnetic performance. It has been shown that to obtain the optimum electromagnetic performance with a coated rotor, the thickness of the coating material must be around 1.5 mm, irrespective of the rotor's diameter [7]. This thickness is enough to provide the magnetic benefits, while a thicker coat would adversely affect the motor's performance. In

addition, the conductivity of the coating materials must be twice that of the rotor material [3].

In this study the high-speed performance of the four different types of rotor mentioned above (and which have the same geometrical quantities) is presented using a finite-element analysis (FEA). The number of turns per stator slot is selected so as to obtain the same stator current in rated operation. All four motors were analyzed using FEA tools for 20 different speeds in order to obtain the combined torque-speed characteristics. To illustrate visually the differences in the distributions of the magnetic flux and the eddy current the results for 11300 rpm are presented and the core loss, the total loss and the efficiency for the specific speed are compared for all the motors. This paper complements another paper by the same authors [8], where we propose an innovative and more efficient solid rotor type for the same rated speed.

2. 2D Transient Magnetic Model

In order to obtain the performance characteristics for the different rotor types as part of the comparison, a conventional squirrel-cage (cage rotor) induction motor (CRIM) was used as a reference with its geometrical quantities. Three solid-rotor induction motors were designed for the comparison, i.e., a Smooth Solid-Rotor Induction Motor (Smooth-SRIM), a Slitted Solid-Rotor Induction Motor (Slitted-SRIM) and a Copper-Coated Rotor Induction Motor (CCSRIM). All three motors have the same stator core as the CRIM, while the number of turns per slot is optimized to keep rated stator current constant.

2.1. Cage-Rotor Induction Motor (CRIM)

The operating and geometrical quantities of the reference conventional squirrel-cage (cage rotor) induction motor (CRIM) are given in Table I and the 2D transient magnetic model is illustrated Fig. 1.

Table 1. Parameter of the Cage-Rotor Induction Machine (CRIM)

Symbol	Quantity	Value
P	Rated output power	4 kW
V/f	Rated voltage/frequency	380 V/50 Hz
I	Rated current	8 A
n_r	Rated speed of rotor	2870 min^{-1}
Q_s	Number of stator slots	36
Q_r	Number of rotor slots	28
D_i	Inner diameter of stator	0.08m
D_{out}	Outer diameter of stator	0.15m
D_2	Diameter of rotor	0.0794m
L_i	Total length of rotor	0.10m
k_{fe}	Stacking factor	0.94

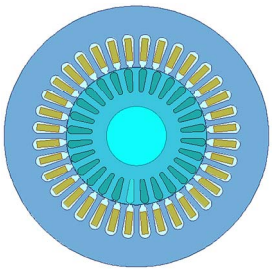

Fig. 1. 2D Transient magnetic model of caged-rotor induction motor

2.2. Smooth Solid-Rotor Induction Motor (Smooth-SRIM)

The solid-rotor induction motor (SRIM) concept is based on the need to build a cheaper and more reliable IM. Even though the production of the rotating field and the stator core's design are the same as that of the other IMs, the magnetic, thermal and mechanical performance and rotor current density need to be investigated thoroughly for an efficient design [9][10].

The modeled rotor for the study is a simple, cylindrical shape and is made from 1010 steel. This type of rotor is the strongest of all the solid rotor types in terms of its resistivity to centrifugal force. Since this solid rotor is heavily influenced by the skin effect, a skin-depth-based mesh algorithm is used on the rotor surface in order to obtain more accurate results for the three solid rotor types. The 2D transient magnetic model and the structure of the mesh are given in Fig. 2

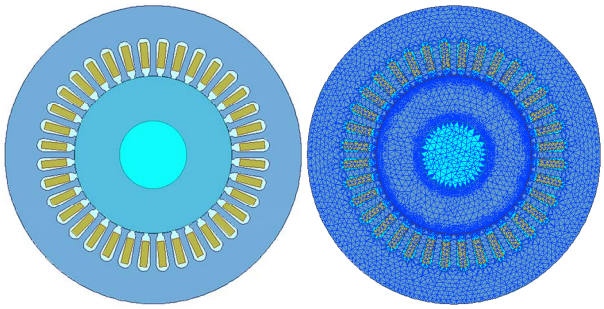

Fig. 2. 2D Transient magnetic model of Smooth-SRIM and its skin-depth mesh structure

The resistivity of the rotor material is multiplied by the end-effect factor (k_e) in order to take the rotor's end-effects into account, and which are calculated as in (1), where ρ_R is the resistivity of the rotor material, ρ_R' is the equivalent resistivity including the end-effect, (2) defines the end-effect factor, while introducing the C coefficient depending on the type of material (which is 0.3 for thick copper end-rings). The coefficient α is presented in (3), where k_R is the Russell factor [6], τ_p is the pole pitch in meters, and l_{Fe} is the active length of the rotor.

$$\rho_R' = k_e.\rho_R \tag{1}$$

$$k_e = 1 + C.(\alpha - 1) \tag{2}$$

$$\alpha = \frac{1}{k_R} = \frac{1}{1 - \frac{2.\tau_p}{\pi.l_{Fe}} \tanh\left(\frac{\pi.l_{Fe}}{2.\tau_p}\right)} \quad (3)$$

2.3. Axially Slitted Solid-Rotor Induction Motor (ASSRIM)

The axially slitted rotor induction motor (ASSRIM) effectively reduces the rotor losses caused by the air-gap harmonics [5]. Depending on its structure, the ASSRIM utilizes the active material more effectively than the Smooth-SRIM [11]. One of its primary features is its relatively smaller inertia [12].

To optimize the electromagnetic performance of a slitted rotor, the slit width and depth need to be 2 mm and half of the rotor's radius, respectively [6]. The designed slitted rotor's properties are given in Table 2. A skin-depth mesh is also used to obtain better skin-effect results. The 2D transient magnetic model and the mesh structure are illustrated in Fig. 3.

Table 1. Geometrical properties of the modeled ASSRIM

Quantity	Value
Number of Slits	28
Angle between two slits	12.85°
Slit length	19.85
Slit width	2 mm

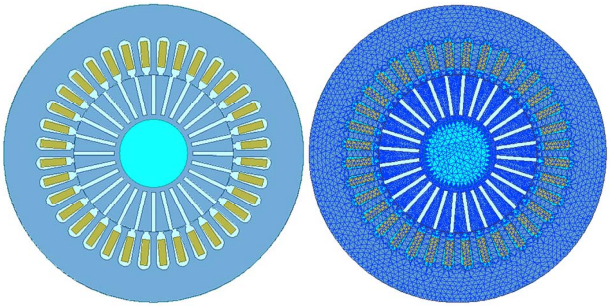

Fig. 3. 2D Transient magnetic model of the ASSRIM and its skin-depth mesh structure

2.4. Copper-Coated Solid-Rotor Induction Motor (CCSRIM)

The coating reduces the effect generated by the air-gap harmonics, increasing the motor's electromagnetic performance. The large thermal-conductivity property is more important than the electrical resistivity of the coating material [13]. Nevertheless, a high electrical conductivity provides fewer rotor losses than a low electrical conductivity. The highly conducting material covering the rotor acts as buffer for the high-frequency air-gap mmf harmonics and prevents them from penetrating deep into the rotor core, while providing an increase in the electromagnetic torque production.

In this part of the study, copper is used as a coating material, since it is the second-best conducting material with 59.6×10^6 S/m, while providing a high thermal conductivity, which is excellent for a coating material [14]. The end-effect factor needs to be used again and the equivalent coefficient for both copper and steel must be calculated by using (1), (2) and (3) for the coated rotor, which is different than for the Smooth-SRIM [4]. A 2D FEA cannot take the end-ring effect into account using the Russell correction factor [4].

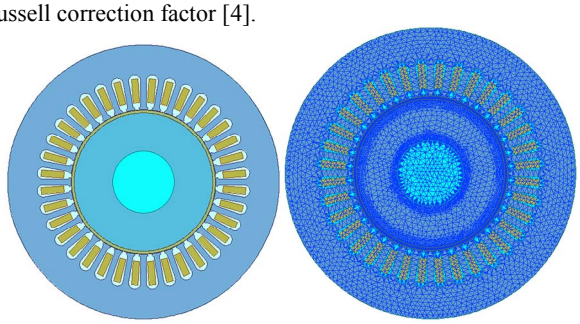

Fig. 4. 2D transient magnetic model of CCSRIM and its skin depth mesh structure

Thickness of the coating material is 1.5 mm in the 2D transient magnetic model in order to improve the electromagnetic performance of the motor [7]. The skin-depth mesh is also used to obtain better skin-effect results. The 2D transient magnetic model and the skin-depth mesh structure are presented in Fig. 4.

3.Results

To compare the torque-speed characteristics of all four motors, each motor was analyzed for numerous different speeds between 0 and 12000 min^{-1}, and then the combined characteristics were obtained. In order to make a visual comparison for all the designs, only one simulation result for each design, including the magnetic flux density, the magnetic flux lines and the eddy-current density distributions, is presented for 11300 min^{-1} using a 5.8 % slip value.

The magnetic flux densities of the different types of motors are given in Fig. 5, 6, 7, and 8. The magnetic flux line distributions for the different types of motors are given in Fig. 9, 10, 11, and 12.

The rotor-current density of the caged rotor and the eddy-current density of the other types of rotors can be seen in Fig. 13, 14, 15, and 16.

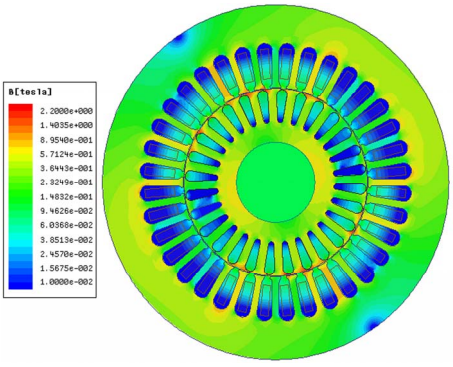

Fig. 5. Magnetic flux density of CRIM

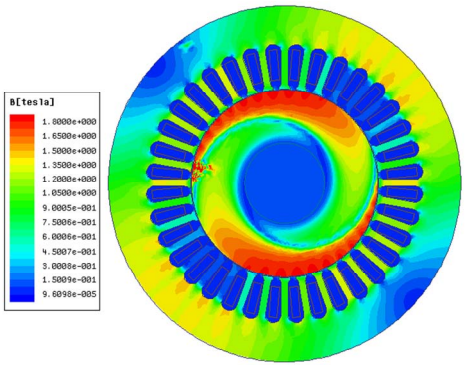

Fig. 6. Magnetic flux density of Smooth-SRIM

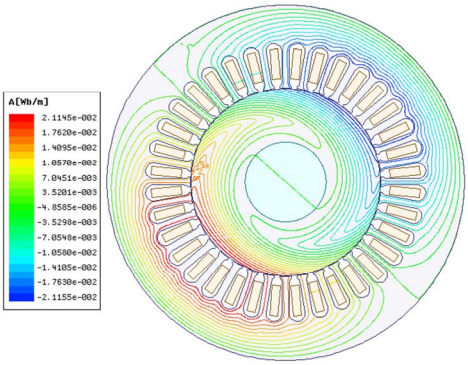

Fig. 10. Magnetic flux lines of Smooth-SRIM

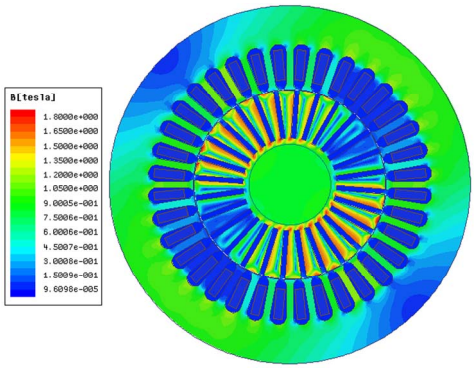

Fig. 7. Magnetic flux density of ASSRIM

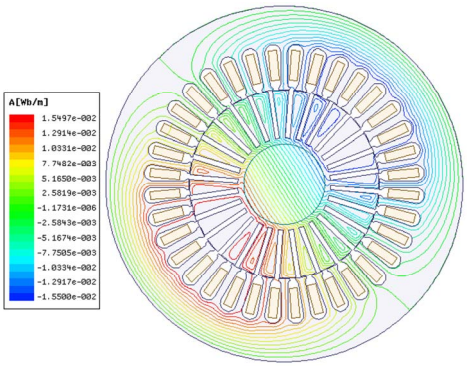

Fig. 11. Magnetic flux lines of ASSRIM

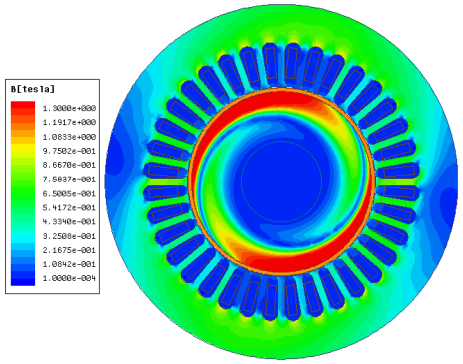

Fig. 8. Magnetic flux density of CCSRIM

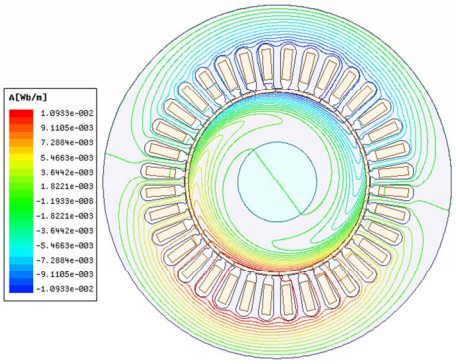

Fig. 12. Magnetic flux lines of CCSRIM

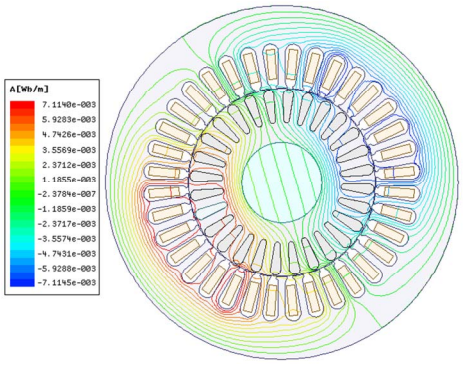

Fig. 9. Magnetic flux lines of CRIM

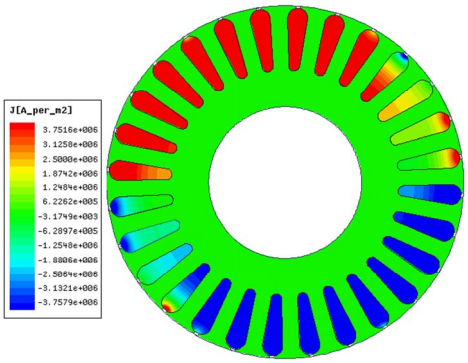

Fig. 13. Rotor-current density of CRIM

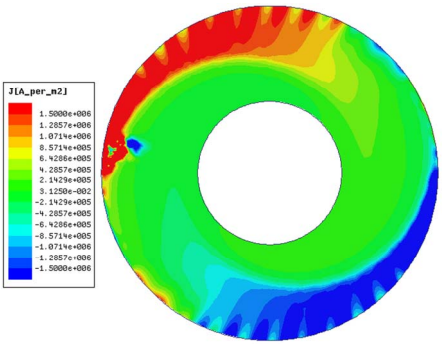

Fig. 14. Rotor-current density of Smooth-SRIM

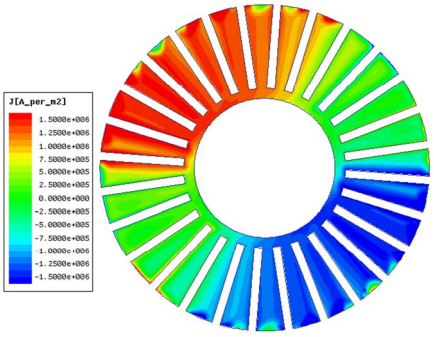

Fig. 15. Rotor-current density of ASSRIM

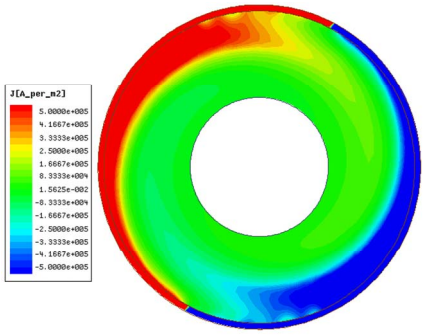

Fig. 16. Rotor-current density of CCSRIM

The torque-speed characteristics of the analyzed motors with different rotor designs are presented in Fig. 17.

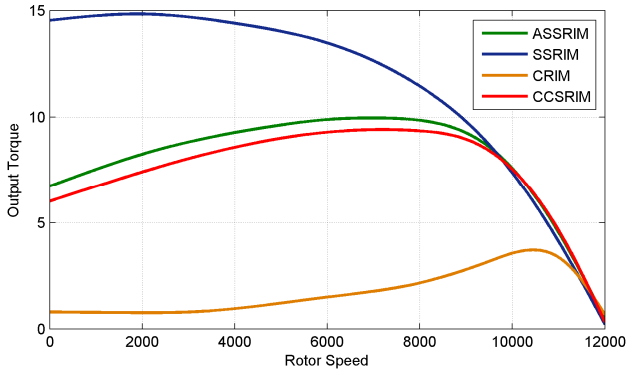

Fig. 17. Torque-speed charakteristics for the different types of rotors

Before interpreting the characteristics, it must be kept in mind that the operating speed is very high for the linear operating zone at approximately 12000 min^{-1}. This provides a tremendous increase in the shaft power when the rotor speed is increased by a small value.

As is clear from Fig 17, the high-speed operation of the Smooth-SRIM is the worst in terms of electromechanical energy conversion, in addition to its structural disadvantages. The CCSRIM is the highest torque-producing type at a certain speed, providing the highest shaft power, although it has a lower pull-out torque than that of the ASSRIM and the Smooth-SRIM.

It is clear from Fig 5-16 that the flux lines have problems in penetrating deep into the rotor core for all the designs, depending on the operating frequency. It is obvious that the cage rotor has electromagnetic disadvantages, in addition to its electromechanical and structural disadvantages for high-speed applications. The Smooth-SRIM has better magnetic performance than the CRIM, but slitting and coating increases the magnetic performance of the rotor core, bringing about an increase in rotor's mechanical performance.

Using different designs not only leads to a durable design with a better magnetic, electromechanical performance, but also a better operating performance, producing fewer losses with greater efficiency. Comparisons of the rotor-core losses, the total losses and the efficiency for all the designs are given in Fig 18-20, respectively.

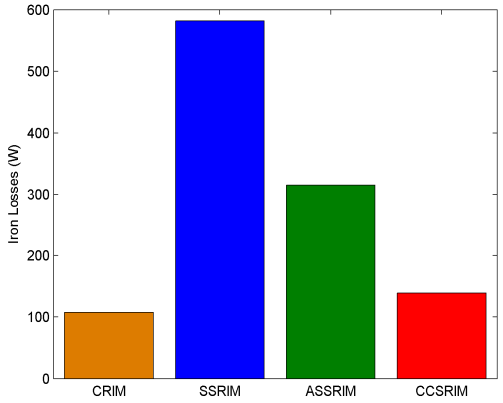

Fig. 18. Core-loss comparison for different types of rotors

Fig. 18-20 shows that the CRIM is a better choice in terms of higher efficiency and fewer losses

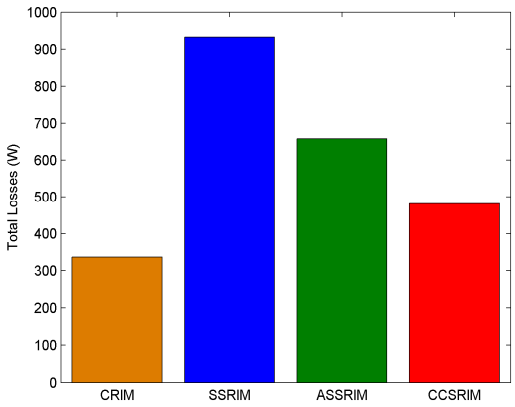

Fig. 19. Total-loss comparison for the different types of rotors

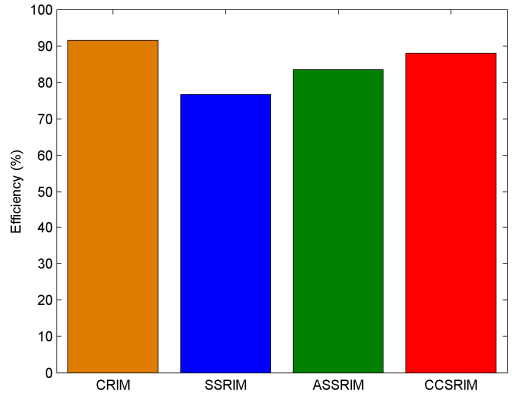

Fig. 20. Efficiency comparison for the different types of rotors

However, it must be taken into account that the mechanical and thermal properties of the rotor were not investigated. During high-speed operation the rotor is affected by centrifugal forces and requires more ventilation to maintain its high thermal durability. The centrifugal force and the thermal weakness of the rotor increase with the angular velocity. These effects show that the CRIM's structural robustness is not sufficient for the task in high-speed applications.

The CRIM's high efficiency and low losses will not contribute to its operation in high-speed industrial applications, since the CRIM has the worst torque-speed characteristic with its low pull-out torque, fast-changing rotor speed with the load and a weak structure. The SRIM types have more mechanical advantages than the CRIM. The lowest core loss and total loss, and the highest efficiency belong to the CCSRIM for all three SRIM types. These designs not only improved the thermal properties and the mechanical integrity, but are also easier to manufacture.

4. Conclusion

In this study the performances of four different types of rotors, i.e., cage, smooth solid, slitted solid and coated solid, were investigated for high-speed drive applications. First, basic information about the four different rotor types is presented. All the 2D transient magnetic models for the high-speed induction motors were built up using a FEA tool. All the motors with their different rotor types had the same stator core, but with different numbers of turns per slot. The other geometrical properties were kept the same. All the motors were analyzed for numerous speeds and the integrated torque-speed characteristics were obtained and compared.

The distribution of the magnetic flux density, the magnetic flux lines and the distributions of the eddy-current densities of all the rotor types were presented. The core loss, the total loss and an efficiency comparison for the different type of rotors are described.

Although the CRIM has a higher efficiency and the fewest losses, its mechanical output is not as high as the other analyzed motors. All the SRIMs provide more output power and torque for high-speed applications. Of the SRIM types, the CCSRIM exhibits the best torque-speed output for high-speed applications, with the lowest core loss and total loss, and the highest efficiency, in addition to its well-known physical and thermal capabilities.

7. References

[1] Jokinen, 1988 Jokinen, T. "High-speed electrical machines", Conference on high speed technology, Lappeenranta, Finland, 1988, pp. 175-185. J.

[2] L. Papini, C.Gerada, D. Gerada, Abdeslam Mebarki, "High Speed Solid Rotor Induction Machine: Analysis and Performances", 2014, 17th İnternational Conference on Electrical Machines and Systems (ICEMS), Oct. 22-25, 2014, Hangzhou, China

[3] T. Aho, J. Nerg and J. Pyrhönen, "Analyzing the Effect of the Rotor Coating on the Rotor Losses of Medium-Speed Solid-Rotor Induction Motor", International Symposium on Power Electronics, Electrical Drives, Automation and Motion (SPEEDAM) 2006

[4] J. Klima, O. Vitek, "Anaysis of High-Speed Induction Motor"

[5] Pyrhönen J. and Huppunen J.: "A New Medium Speed Solid Induction Motor for a High-Speed Milling Machine", Proceedings of 1996 Symposium on Power Electronics, Industrial Drives, Power Quality, Traction Systems (Speedam ´96). pp. B5-1 - B5-7. Capri, Italy, 1996.

[6] Mekuria, "Developement of a high speed solid rotor asynchronous drive fed by a frequency converter system" PhD Thesis, 2013, Technical University of Darmstadt, Germany

[7] K. Tatıs, A. Kladas And J.Tegopoulos, "Solid Rotor Induction Machine Optimisation based on Finite Element Techniques"

[8] D. T. McGuiness, M. O. Gulbahce, D. A. Kocabas, "Novel Rotor Design for High-Speed Solid Rotor Induction Machines", *9th International Conference on Electrical and Electronics Engineering (ELECO)*, 2015

[9] Papini, L.; Gerada, C., "Thermal-electromagnetic analysis of solid rotor induction machine," Power Electronics, Machines and Drives (PEMD 2014), 7th IET International Conference on, vol., no., pp.1,6, 8-10 April 2014.

[10] Borisavljevic, A; Polinder, H.; Ferreira, Braham, "Overcoming limits of high-speed PM machines, "Electrical Machines, 2008. ICEM 2008. 18th International Conference on , vol., no., pp.1,6, 6-9 Sept.2008

[11] S. Kubzdela, and B. Weglinski, "Magnetodielectrics in induction motors with disk rotor," IEEE Trans. on Magn, vol. 24, No. I, pp. 635-638, 1988.

[12] M. Mirzayee, M. Mirsalim, and S.B. Abdollabi, "Analytical modeling of a disk induction motor using maple software," ISTET'03, CD Proceeding, Warsaw, Poland, 2003.

[13] J. Huppunen, "High-speed solid-rotor induction machine: electromagnetic calculation and design", PhD Thesis, Lappeenranta: Lappeenrannan Teknillinen Yliopisto, 2004. ISBN 95-176-4981-9.

[14] Hammond, C. R. (2004). The Elements, in Handbook of Chemistry and Physics (81st ed.). CRC press. ISBN 0-8493-0485-7.

[15] T. Aho, J. Nerg, J. Pyrhonen, "Experimental and finite element Analysis of solid rotor End effect", Lappeenranta University of technology, Department of Electrical Engineering, IEEE, 1242-1245 p.

[16] J. Gieras and J. Saari, "Performance calculation for a high-speed solidrotor induction motor," Industrial Electronics, IEEE Transactions on, vol. 59, no. 6, pp. 2689–2700, 2012.